Available online at www.sciencedirect.com
ScienceDirect
Journal of Nuclear Materials 374 (2008) 9–19
journal of nuclear materials
www.elsevier.com/locate/jnucmat

Characterization of $(Th,U)O_2$ fuel pellets made by impregnation technique

T.R.G. Kutty [a,*], M.R. Nair [a], P. Sengupta [b], U. Basak [a], Arun Kumar [a], H.S. Kamath [c]

[a] Radiometallurgy Division, Bhabha Atomic Research Centre, Trombay, Mumbai 400 085, India
[b] Materials Science Division, Bhabha Atomic Research Centre, Trombay, Mumbai 400 085, India
[c] Nuclear Fuels Group, Bhabha Atomic Research Centre, Trombay, Mumbai 400 085, India

Received 15 December 2006; accepted 9 July 2007

Abstract

Impregnation technique is an attractive alternative for manufacturing highly radiotoxic ^{233}U bearing thoria based mixed oxide fuel pellets, which are remotely treated in hot cell or shielded glove-box facilities. This technique is being investigated to fabricate the fuel for the forthcoming Indian Advanced Heavy Water Reactor (AHWR). In the impregnation process, porous ThO_2 pellets are prepared in an unshielded facility which are then impregnated with 1.5 molar uranyl nitrate solution in a shielded facility. The resulting composites are dried and denitrated at 500 °C and then sintered in reducing/oxidizing atmosphere to obtain high density $(Th,U)O_2$ pellets. In this work, the densification behaviour of ThO_2–2% UO_2 and ThO_2–4% UO_2 pellets was studied in reducing and oxidizing atmospheres using a high temperature dilatometer. Densification was found to be larger in air than in Ar–8% H_2. The characterization of the sintered pellets was made by optical microscopy, scanning electron microscopy (SEM) and electron probe microanalysis (EPMA). The grain structure of ThO_2–2% UO_2 and ThO_2–4% UO_2 pellets was uniform. The EPMA data confirmed that the uranium concentration was slightly higher at the periphery of the pellet than that at the centre.

PACS: 81.20.Ev; 61.72.−y; 66.30.Fq; 62.20. Fe; 81.70.P

1. Introduction

The technology of fabrication of Pu-bearing uranium fuels like MOX for both LWR's or FBR's has now been mastered industrially by many countries. Generally, the large scale production of MOX fuel pellets is carried out by sintering the green compacts in a reducing atmosphere at high temperatures around 1700 °C [1,2]. However, when the fabrication of fuels containing highly radioactive materials, such as ^{233}U, americium, curium, long-lived fission products or transmutation nuclides is considered, the production of dust and consequent radiation exposure to personnel could restrict the use of the above usual process consisting of co-milling, cold compaction and sintering. Therefore, alternative fabrication routes that are more amenable for remotization and automation procedures are being considered [3–6]. Some of the promising methods other than powder pellet route are (a) sol–gel microsphere pelletization (b) vibro-sol route and (c) impregnation technique [7]. Among them, the impregnation technique is an attractive alternative for manufacturing highly radiotoxic ^{233}U bearing thoria based mixed oxide fuel pellets [8–10]. In this process, low density pellets ($\leqslant$75% T.D.) with open porosity are first prepared in an unshielded area. The ThO_2 pellets thus prepared are impregnated in uranyl nitrate (^{233}U) solution followed by sintering to obtain ThO_2-based mixed oxide pellets of high density and good microhomogeneity [7]. That is to say, handling of fine ^{233}U bearing powders in remote facilities can be avoided. Another advantage of this process is that it can be coupled with the reprocessing plant so that the purified feed from

* Corresponding author. Fax: +91 22 2550 5151.
E-mail address: tkutty@barc.gov.in (T.R.G. Kutty).

0022-3115/$ - see front matter © 2007 Elsevier B.V. All rights reserved.
doi:10.1016/j.jnucmat.2007.07.004

ion exchange columns may be straightway used as the infiltrant [7–10]. The impregnation process can thus simplify the fuel reprocessing operation and eliminate several expensive stages from operations. As no precipitation or washing steps are required within the shielded area, the amount of radioactive wastes produced in the process is small [9,11].

Thorium fuel cycle contributes to produce long term nuclear energy with a small amount of radiotoxic waste. The fuel not only reduces plutonium production but also reduces the formation of highly radioactive isotopes [12–16]. Regarding to waste management, the Th containing fuel creates more ^{129}I and ^{234}U due to higher amount of ^{233}U in it. However, the U fuel forms more ^{99}Tc, ^{237}Np and ^{239}Pu and some heavier actinides [17,18]. The amount of thorium in the earth crust is estimated to be three times that of uranium. India has vast thorium reserves (five times that of uranium) in contrast to modest quantity of uranium. The currently known Indian thorium reserves amount to 358 000-GWe year of electrical energy, which can easily meet the energy requirements during the next century and beyond [19]. Accordingly, while formulating the national programme, thorium has been envisaged as the fuel for the third and the largest phase of Indian nuclear power programme. India is currently engaged in the design of a thorium fuelled advanced heavy water reactor (AHWR) for generation of power. The AHWR is being developed in India with the specific aim to utilize thorium for power generation. AHWR is a 300 MWe, vertical, pressure tube type reactor cooled by boiling light water and moderated by heavy water. It incorporates several advanced passive safety features, e.g., heat removal through natural circulation [20,21]. The AHWR fuel comprises a 54 pin composite fuel cluster containing 24 (Th–Pu)O_2 pins and 30 (Th–^{233}U)O_2 pins. Fabrication of (Th–^{233}U)O_2 mixed oxide fuel is, however, not easy because it usually contains daughters of ^{232}U (half-life 73.6 years) namely, ^{212}Bi and ^{208}Tl which emit strong gamma radiations of 0.7–1.8 MeV and 2.6 MeV, respectively. Therefore the fabrication of above fuel requires operations in shielded glove-boxes to protect the operators from radiation. The aim of this work is to develop the impregnation technique to fabricate ThO_2–2% UO_2 and ThO_2–4% UO_2 fuel pellets. The mixed oxide of ThO_2 containing ~4% $^{233}UO_2$ is the proposed fuel for the AHWR and ThO_2–2% $^{233}UO_2$ is considered as an alternative fuel for thermal reactors. In this study, natural U has been used as a surrogate for ^{233}U.

The objectives of this study are listed below:

1. Fabrication study of high quality ThO_2–UO_2 pellets by impregnating ThO_2 with uranyl nitrate solution.
2. Evaluation of shrinkage behaviour of ThO_2–2% UO_2 and ThO_2–4% UO_2 compacts in the atmospheres of Ar–8% H_2 and air.
3. Study of the microstructural features of the pellets of the above compositions.
4. Investigation of uranium distribution in the above pellets after sintering.
5. Search of alternate method to produce the mixed oxide pellets which is more economic with minimum processes of handling of highly toxic or radioactive materials in shielded environment.

2. Impregnation technique

The impregnation technique of Bhabha Atomic Research Centre (BARC) is very similar to infiltration of radioactive materials (INRAM) [22–29] which has recently been applied for Am target fabrication. The process relies on the action of capillary forces to draw the solution into the pores of the host material. The amount of the second material introduced into the pellet can be controlled by adjusting the concentration of the infiltrant solution. The only requirement for the application of this process to the fabrication of fuel pellet is that the pellet should be insoluble in the solution containing the infiltrant and that the infiltrant can be easily convertible into the desired chemical form [9,11]. It is important that many of the porosities are interconnected and distributed uniformly across the pellet otherwise the impregnation will not be effective. Use of microwave during impregnation for local heating of the partially sintered low density pellets has been tested for expulsion of entrapped gas to accelerate impregnation. For uniform distribution of actinide in the sintered pellets, annular pellets are more suitable than the conventional ones. The concentration of the added material can be increased by multiple impregnation or by the use of the solution containing higher concentration of the material.

The flow-sheet of fabrication of ThO_2–4% UO_2 pellets by impregnation process is given in Fig. 1. The procedures for the fabrication of ThO_2–UO_2 pellets followed by Bhabha Atomic Research Centre (BARC) involve the following steps [30]:

1. Fabrication of low density (~66% T.D.) ThO_2 pellets by powder route in an unshielded facility.
2. Impregnation of the above pellets by uranyl nitrate solution under vacuum in a shielded facility.
3. Drying and final sintering at 1700 °C in reducing atmosphere.

The U loading in ThO_2 pellet can be varied by controlling the following parameters such as:

(a) Density of the pre-sintered ThO_2 pellets.
(b) Concentration of uranyl nitrate solution.
(c) Duration of impregnation.

3. Experimental

3.1. Preparation of green compacts

The ThO_2–2% UO_2 and ThO_2–4% UO_2 green pellets for this study are prepared as described in Section 3.2 by the impregnation process. The characteristics of the

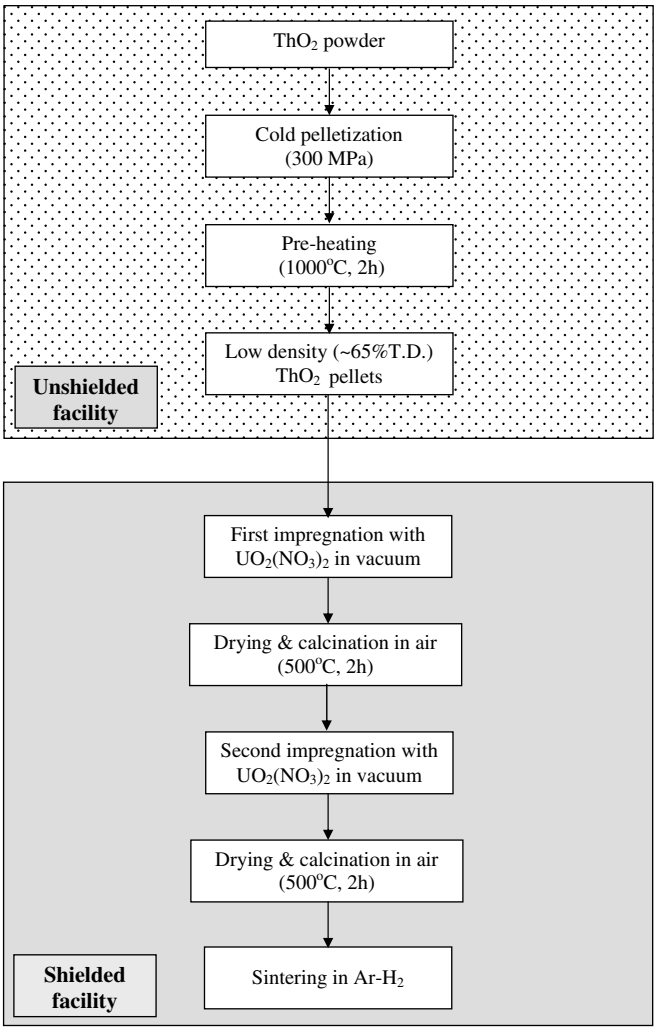

Fig. 1. The flow-sheet of fabrication of ThO_2–4% UO_2 pellet by impregnation process.

starting ThO_2 powders used in this study are given in Table 1. ThO_2 powders used in this study had 500 ppm of MgO as sintering aid. These powders were milled in a planetary ball for 2 h and then doubly precompacted at 75 and 150 MPa into pellets. This is followed by granulation. These granules were used to make pellets by compacting them at 300 MPa. The green density of the compacts was in the range of 63–65% of the theoretical density. The pellets were about 8 mm in diameter and around 10 mm in length. Some ThO_2 green compacts were not impregnated with uranyl nitrate solution and used as control samples.

Table 1
Basic characteristics of starting ThO_2 powders

BET surface area (m^2/g)	3.72
Apparent density (g/cm^3)	1.23
Tap density (g/cm^3)	2.28
Total impurity (ppm)	<1000

3.2. Impregnation

The density of the host pellets (ThO_2) was optimized by changing the pre-sintering temperature. ThO_2 green pellets were pre-sintered at 600, 1000, 1150 and 1200 °C to obtain the pellets of various densities ranging from 6.3 g/cm^3 to 7.5 g/cm^3. By conducting experiments using the host pellets of different densities, it was observed that the pellet of 6.6 g/cm^3 density (pre-sintered at 1000 °C for 2 h) gave the most satisfactory result. The pre-sintered pellets were immersed in 1.5 M uranyl nitrate solution under the controlled vacuum. The pellets were kept in the liquid for about 1 h to complete impregnation. In this study the concentration of uranyl nitrate solution was not changed from 1.5 M. After impregnation, the pellet was dried and then calcined at 500 °C for 2 h. The amount of uranium impregnated in ThO_2 was found to be around 2% from the weight gain of the pellet after the calcination. Attempts to increase the uranium amount by increasing the porosity of ThO_2 pellet using pore formers (methyl cellulose) did not give good results because such pellets were insufficient in strength to withstand the liquid impregnation. A series of experiments were conducted with batch sizes ranging from 250 g to 5 kg with 1.5 M uranyl nitrate solution. In all the above experiments, the uranium concentration in ThO_2 was around 2%. For having ThO_2–4% UO_2 pellet, then, the above pellet was again impregnated with 1.5 M uranyl nitrate solution and calcined at 500 °C for 2 h.

3.3. Dilatometry

The shrinkage behaviour of ThO_2, ThO_2–2% UO_2 and ThO_2–4% UO_2 pellets was studied using a high temperature dilatometer. The dilatometry was carried out under the following condition:

- force on the sample 0.2 N,
- gas flow 12 l/h and
- heating rate 6 K/min.

The measurements made using a Netzsch (model 402E) horizontal dilatometer. The dilatometric data were obtained are in the form of curves of dimension against time and temperature. Here, the sample rests between the push rod and stopper. The length change is transmitted through the frictionless push rod to an LVDT transducer. The accuracy of the measurement of change in length was within ±0.1 μm. A calibrated thermocouple was placed just above the sample to record the sample temperature. The dilatometric experiments were carried out in reducing (Ar–8% H_2) and oxidizing (air) atmospheres. The impurity contents of the cover gases used in this study are given in Table 2. The selection of the temperature programme was made by a computer via the data acquisition system. The shrinkage of a standard sample (POCO graphite, NIST) was measured under identical condition in order to correct for the differences in shrinkage between the sample holder

Table 2
Impurity contents in the sintering atmospheres (volume ppm)

Sintering atmosphere	Oxygen (vppm)	Moisture (vppm)	CO_2 (vppm)	CO (vppm)	N_2 (vppm)	Oxides of N_2 (vppm)	Hydrocarbon (vppm)
Argon + 8% hydrogen	4	4	1	1	10	1	2
Air	Bal	10	5	0	Bal	1	1

and the sample. Table 3 gives the typical impurity contents of a sintered pellet. The density and O/M (M = Th + U) ratio of the pellets covered in this study are shown in Table 4.

3.4. Characterization

The ThO_2, ThO_2–2% UO_2 and ThO_2–4% UO_2 pellets were characterized by the following techniques:

- XRD.
- Density.
- Metallography.
- Thermogravimetry.
- SEM.
- EPMA.

The O/M ratio and XRD data were obtained for the samples after sintering. The O/M ratio of the sintered pellet was measured thermogravimetrically using Bahr (Model STA-503) thermal analyzer. The accuracy of the measurement in weight was within ±1 μg. The O/M ratio of the sample heated in air was obtained from the weight decrease of this sample on heating in Ar–8% H_2 at 800 °C of which the O/M ratio is 2.00. The phase analysis was performed using X-ray diffractometry (Diano make, model XRD-8760) and metallography (Leica make, model Polyvar microscope). The X-ray diffraction patterns of the pellets were obtained by using Cu Kα radiation monochromatized with curved graphite monochromator. The accuracy of this equipment is ±5%. The green density was measured geometrically and the sintered density was determined following the Archimedes method (Mettler Toledo, model SAG 105). For metallography, the pellets sintered in Ar–8% H_2 and air were mounted in Araldite cement and ground using successive grades of emery papers. The final polishing was done using diamond paste. The pellet was then removed from the mount by dissolving the cement by acetone and then etched thermally by holding it at 1500 °C for 4 h in air. The grain size was determined by the intercept method. The microstructure was characterized by SEM (Philips make, model XL-30). The uranium distribution in the sintered pellet was determined by EPMA (Cameca, model Sx-100).

Table 3
Metallic impurities in a typical sintered pellet made by impregnation process

Element	Impurity (ppm)
Na	14
Al	9
Mg	410
Si	<110
Fe	20
Cr	<1
Co	<5
Ni	<1
Mo	<5
W	<50
Cu	1.0
B	<0.6

Table 4
Densities and O/M ratios of the sintered ThO_2–UO_2 pellets heated in oxidizing and reducing atmospheres

Composition	Density (% TD)		O/M ratio	
	Air	Ar–8% H_2	Air	Ar–8% H_2
ThO_2	92.9	89	2.000	2.000
ThO_2–2% UO_2	92.1	87	2.008	2.000
ThO_2–4% UO_2	95.7	87	2.010	2.000

4. Results

Fig. 2 shows the shrinkage behaviour of ThO_2–2% UO_2 and ThO_2–4% UO_2 pellets made by the impregnation route in reducing atmosphere (Ar–8% H_2). The shrinkage behaviour of control sample, ThO_2, is shown together in the same figure. Here dl/l_0 is plotted against temperature,

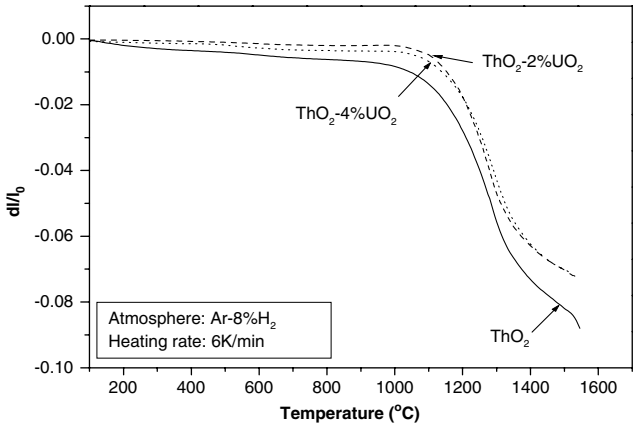

Fig. 2. Shrinkage curves for ThO_2, ThO_2–2% UO_2 and ThO_2–4% UO_2 pellets heated in Ar–8% H_2 atmosphere. Here dl/l_0 is plotted against temperature where l_0 is the initial length.

where l_0 is the initial length of the pellet in the axial direction and dl is its increment. The corresponding shrinkage rates d(dl/l_0)/dt of the above pellet are shown in Fig. 3. From Fig. 2, it is seen that the onset temperature of sintering is around 975 °C for pure ThO_2 while these are about 1050 °C for ThO_2–2% UO_2 and ThO_2–4% UO_2 pellets. The onset temperature of sintering was determined from the dilatometric curve as the point at which it deviates from its horizontal path. Fig. 4 shows a plot of shrinkage versus temperature for these oxides in air. The corresponding shrinkage rates d(dl/l_0)/dt of the above pellets are shown in Fig. 5. The shrinkage curve of ThO_2 lies between those of ThO_2–2% UO_2 and ThO_2–4% UO_2 at temperatures higher than 900 °C. In the pellets studied in this work, ThO_2–4% UO_2 shows the highest shrinkage. From the

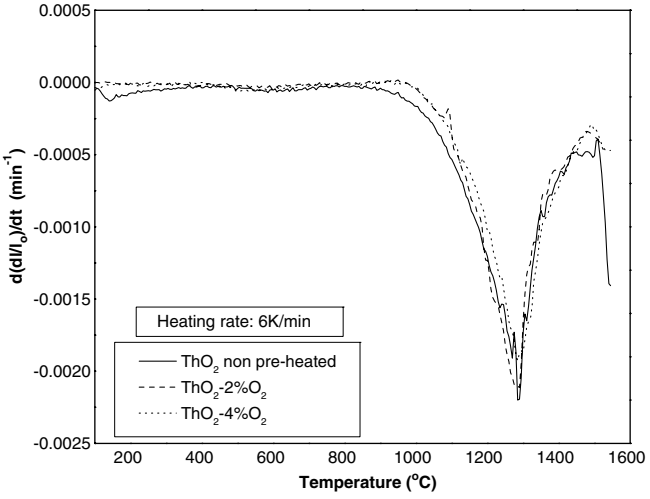

Fig. 3. Shrinkage rate of ThO_2, ThO_2–2% UO_2 and ThO_2–4% UO_2 pellets heated in Ar–8% H_2 atmosphere plotted against temperature.

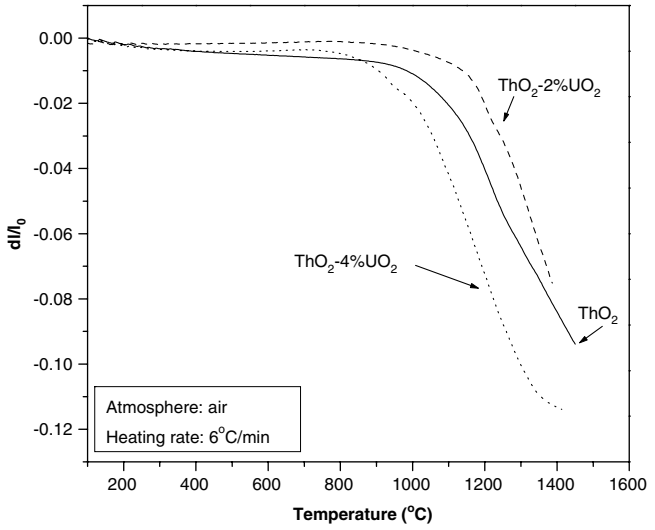

Fig. 4. Shrinkage curves for ThO_2–2% UO_2 and ThO_2–4% UO_2 pellets heated in air. Shrinkage curve for non pre-heated ThO_2 is also shown.

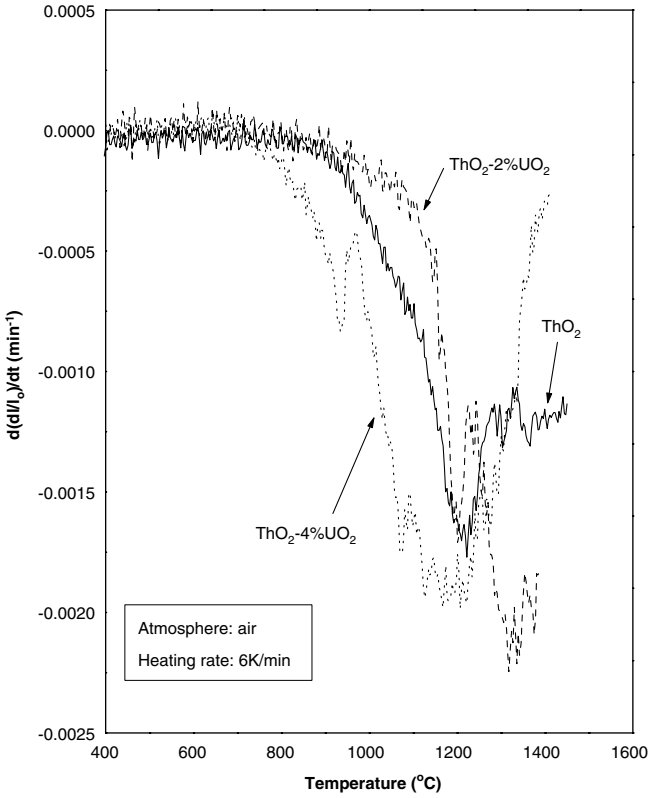

Fig. 5. Shrinkage rate versus temperature for ThO_2, ThO_2–2% UO_2 and ThO_2–4% UO_2 pellets heated in air.

above figures (Figs. 4 and 5), it is seen that the shrinkage occurs above 925 °C in air for ThO_2 and ThO_2–2% UO_2 pellets. For ThO_2–4% UO_2 pellet, the shrinkage was found to commence at a much lower temperature of 800 °C in air. In these pellets, ThO_2–2% UO_2 shows the highest shrinkage rate and ThO_2 shows the lowest in air. The maximum shrinkage rates are observed at 1225, 1325 and 1175 °C for ThO_2, ThO_2–2% UO_2 and ThO_2–4% UO_2, respectively. But for the pellets sintered in Ar–8% H_2, all the above oxides showed the maximum shrinkage rates at the same temperature of 1280 °C (Fig. 3). Fig. 6 compares the shrinkage behaviour of ThO_2–4% UO_2 pellet in reducing (Ar–8% H_2) and oxidizing atmospheres (air). It is evident that the onset temperature of shrinkage in air is much lower (800 °C) than that in Ar–8% H_2.

It is possible to compute the shrinkage levels at two different temperatures from Figs. 2 and 4 and also know the effect of the addition of UO_2 on the shrinkage at a particular temperature. In air at 1300 °C, the shrinkage was 6.5% for pure ThO_2. The shrinkage values were 4.75% and 10.25% for ThO_2–2% UO_2 and ThO_2–4% UO_2, respectively. At the same temperature, the shrinkage in Ar–8% H_2 was 5.5% for pure ThO_2, and the shrinkage values were 4.75% and 4.25% for ThO_2–2% UO_2 and ThO_2–4% UO_2, respectively (Fig. 2).

Fig. 7 shows the microstructures of the ThO_2, ThO_2–2% UO_2 and ThO_2–4% UO_2 pellets. The grain size of

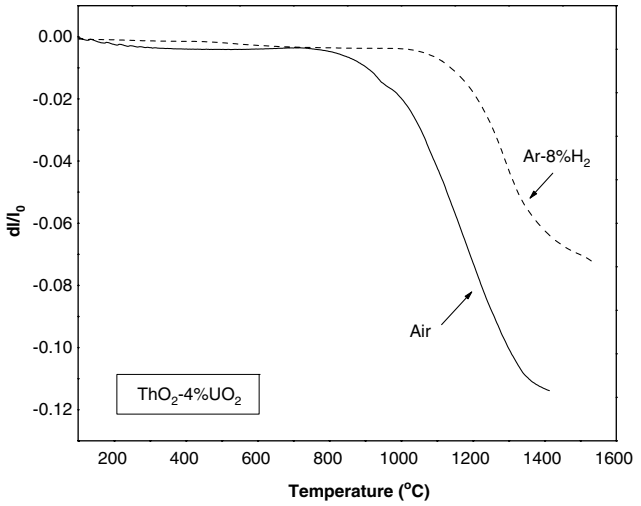

Fig. 6. Shrinkage behaviour of ThO_2–4% UO_2 pellet heated in oxidizing (air) atmosphere compared with that in reducing (Ar–8% H_2) atmosphere.

ThO_2 and ThO_2–4% UO_2 pellets in Fig. 7(a) and (c) does not show large dispersion. The grains are rather uniform. The grains of ThO_2–2% UO_2 pellet (Figs. 7(b)) were also fairly uniform but they were not as well developed as those of the ThO_2–4% UO_2 pellet. The average grain sizes of ThO_2 and ThO_2–4% UO_2 pellets were found to be almost the same (12 μm), and that of ThO_2–2% UO_2 pellet was slightly smaller (10 μm). The XRD data of ThO_2, ThO_2–2% UO_2 and ThO_2–4% UO_2 pellets show that all the above pellets are of single phased. This result was confirmed by metallography. The XRD peaks are found to be sharp indicating that the material is crystalline. The lattice parameter was calculated and was found to be 0.5589 and 0.5587 nm for ThO_2–2% UO_2 and ThO_2–4% UO_2 pellets, respectively. In order to know the distribution of Th, U and O, electron beam scanning was performed by EPMA across the pellet from centre to periphery. A typical result of X-ray intensities of Th Mα, U Mα and O Kα is shown in Fig. 8. It shows the essentially uniform U distribution in the pellet. However, X-ray intensities measured by fixed time counting at various locations show that the U concentration is slightly higher at the periphery than that at the centre for both ThO_2–2% UO_2 and ThO_2–4% UO_2 pellets.

The significant results are summarized below:

1. The grains in the ThO_2–2% UO_2 and ThO_2–4% UO_2 pellets did not show large dispersion in size. They were essentially uniform.
2. The EPMA data confirm that uranium concentration was marginally higher at the periphery of the pellets for both ThO_2–2% UO_2 and ThO_2–4% UO_2.
3. In the atmospheres covered (Ar–8% H_2 and air) in this study, heating in air gave larger shrinkage.
4. The onset temperature of sintering for ThO_2–4% UO_2 pellet in oxidizing atmosphere is lower than that in reducing atmosphere (Ar–8% H_2) by about 200–250 °C.

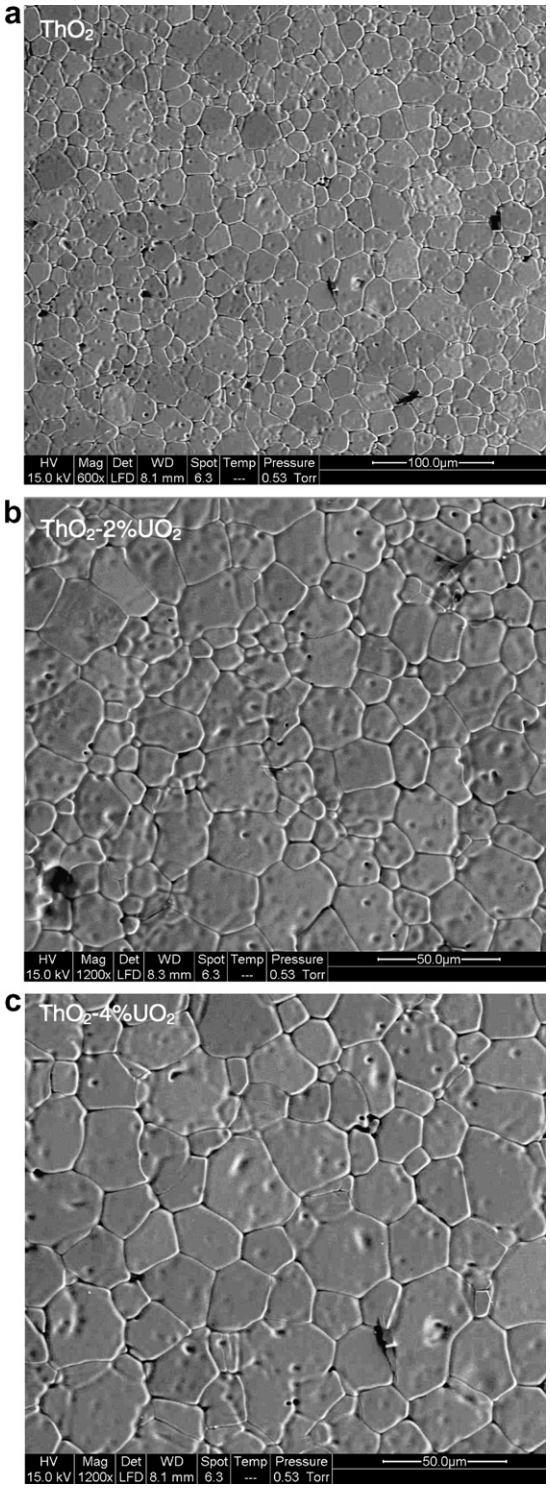

Fig. 7. Microstructure of ThO_2 (a), ThO_2–2% UO_2 (b) and ThO_2–4% UO_2 (c) pellets. These pellets were sintered in air and etched thermally.

5. The maximum shrinkage rate occurred at the same temperature of 1280 °C for all the pellets of the above compositions when sintered in Ar–8% H_2. But the maximum shrinkage rate differed with composition when the pellets were heated in air.

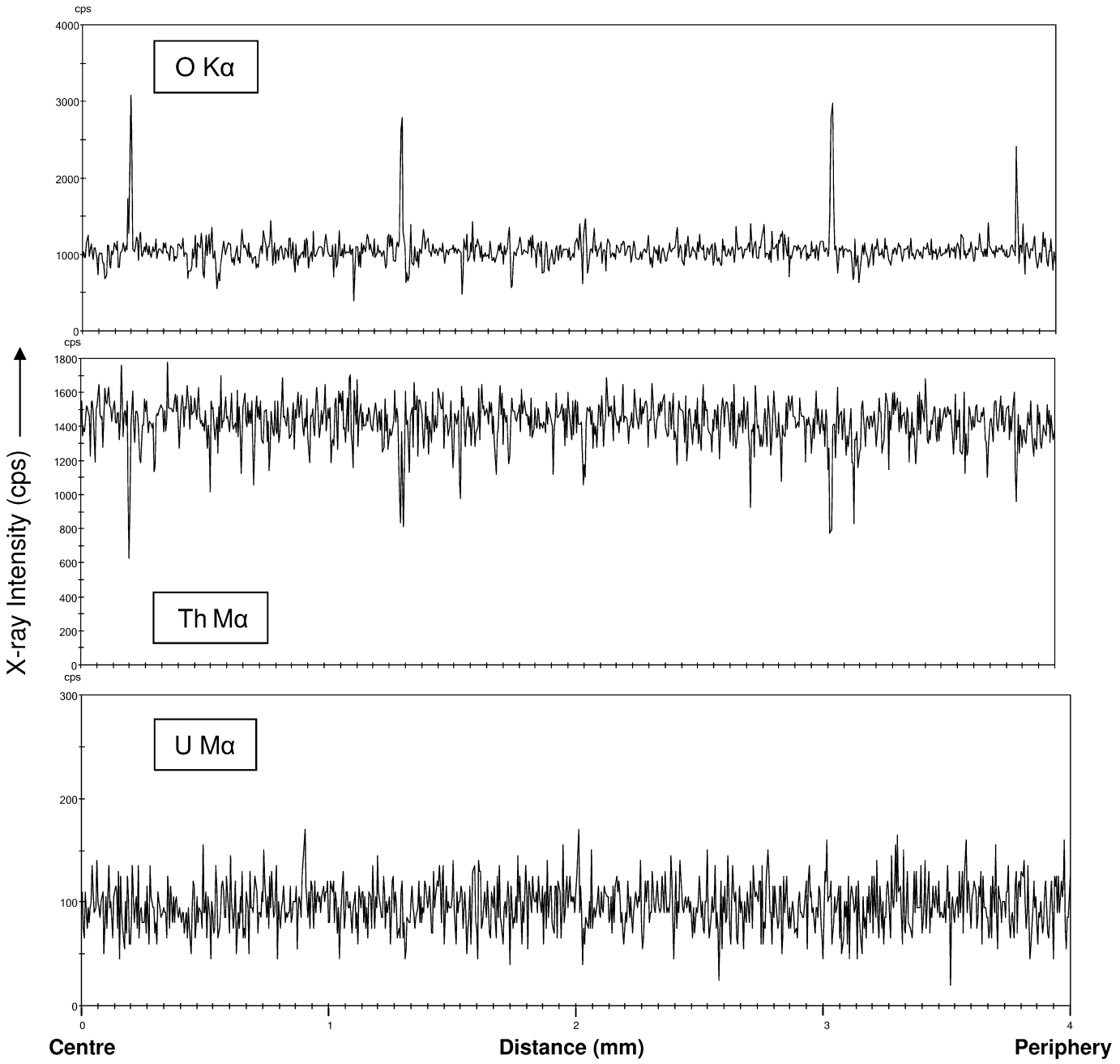

Fig. 8. Typical EPMA line scan for Th Mα, U Mα and O Kα for ThO_2–4% UO_2 pellet. The line scan is taken across the pellet from the centre to the periphery.

5. Discussion

5.1. Densification behaviour

The above results imply that the ThO_2–2% UO_2 and ThO_2–4% UO_2 pellets for thermal reactor fuel could be fabricated using the impregnation technique. In the oxidizing atmosphere, the above pellets gave densities over 92% TD after sintered at 1550 °C. But in the reducing atmosphere, the density was only around 87% T.D. even the pellets were sintered at 1600 °C. Also, the onset temperature of densification was lower in the oxidizing atmosphere than in the reducing atmosphere (Fig. 6). The above difference becomes important for the large scale fabrication of ThO_2–UO_2 sintered pellets since the procedure to sinter in air is economically beneficial without the use of costly cover gases like Ar or Ar–H_2 [31]. Also, costly furnaces with heating elements and sintering boats made of Mo or W are not required.

For nuclear fuel ceramics such as UO_2, it is reported that the diffusion rate is slow under reducing condition and is fast under oxidizing condition. Therefore, a change

in the sintering atmosphere from reducing to controlled oxidizing conditions is very much advantageous to increase the interdiffusion rates [1,2]. Cation mobility increases drastically in hyperstoichiometric oxide because of the large increase in cation vacancy concentration. A low temperature (⩽1300 °C) short time (2 h) sintering has been developed to take advantage of the very high cation mobilities in hyperstoichiometric oxides [1,31]. Since diffusion is largely dependent on oxygen potential of the sintering atmosphere, it will be worthwhile to determine the effects of a variety of atmospheres such as reducing (Ar–8% H_2) and oxidizing (air) atmospheres on the sintering behaviour of ThO_2–UO_2 using a dilatometer.

The sintering is caused by heat treatment of porous specimen without or with the application of external pressure, in which some properties of the pellet are changed with the reduction of the Gibbs free energy to those of the pore-free system. The diffusion of metal atoms depends on concentration of structural imperfections such as metal vacancies. This concentration changes with temperature, atmosphere and dopants [32–41]. The sintering temperature can be lowered either by utilizing appropriate atmosphere or by the addition of dopant. For uranium dioxide, the oxidizing atmosphere has been used for lowering the sintering temperature from 1700 to 1300 °C. In the case of thorium dioxide, dopants have been effectively used for lowering the sintering temperature from 1700 to 1250 °C.

ThO_2 is the only stable solid oxide in the Th–O system, and it has almost no non-stoichiometry. The crystal structure of ThO_2 is the fluorite type, isomorphous with UO_2, PuO_2 and CeO_2, and contains four Th atoms and eight oxygen atoms per unit cell. Th^{4+} is the only one valence state of thorium [42,43]. On the other hand, UO_2 exhibits a wide range of non-stoichiometry at elevated temperatures. This range extends from $UO_{1.65}$ to $UO_{2.25}$ at 2500 °C [1,2]. The hypostoichiometric UO_{2-x} exists only at high temperatures, whereas hyperstoichiometric UO_{2+x} exists even at low temperatures. A typical feature of the fluorite structure is the large (1/2,1/2,1/2) interstitial holes in which the interstitial ions can easily be accommodated [44]. Thus, a large amount of interstitial oxygen can be dissolved causing to form extensive anion excess UO_{2+x}. The charge compensation for the excess of oxygen in UO_{2+x} is achieved by oxidation of U^{+4} to U^{+5} [45]. In this fluorite structure, uranium mobility is many orders of magnitude smaller than oxygen mobility, so that the rate determining step for the diffusion controlled processes such as sintering, grain growth, creep etc. is comprised of uranium diffusion. The ratio of oxygen diffusion coefficient and uranium diffusion coefficient, D^O/D^U, has been reported to be greater than 10^5 at 1400 °C, suggesting that the uranium ion mobility is much smaller than the oxygen mobility. D^U increases in proportion to x^2 by about five orders of magnitude between UO_2 and $UO_{2.2}$ at 1400–1600 °C [31,46,47]. With this background in mind, we will analyze the shrinkage behaviour of ThO_2–UO_2 compacts in Ar–8% H_2 and air below.

5.1.1. Ar–8% H_2

As mentioned in Section 3.1, we used pre-heated ThO_2 compacts for impregnation. The green ThO_2 compacts were heated to 1000 °C in Ar–8% H_2 and held isothermally for 2 h. This pre-heating causes particle coarsening and therefore reduces its sinterability. To study the effect of pre-heating on densification, a pre-heated ThO_2 pellet was heated to 1550 °C in Ar–8% H_2 with a heating rate of 6 K/min. The obtained shrinkage curve is shown in Fig. 9 together with that of ThO_2 pellet which had not been pre-heated. It is seen from the figure that sintering has been retarded by pre-heating. At 1400 °C, the shrinkage was about 7.5% for untreated ThO_2 pellet, and it was 6.5% for pre-heated ThO_2 pellet. The shrinkage of ThO_2 (not pre-heated) was larger than those of pre-heated ThO_2, ThO_2–2% UO_2 and ThO_2–4% UO_2 pellets at all temperatures studied. The shrinkage of ThO_2–2% UO_2 pellet was almost the same as that of ThO_2 pellet, although the latter showed slightly larger shrinkage in the temperature range 1000–1350 °C. The ThO_2–4% UO_2 pellet exhibited larger shrinkage than the pre-heated ThO_2 pellet up to 1300 °C (Fig. 9).

The O/M ratios of both ThO_2–2% UO_2 and ThO_2–4% UO_2 pellets are found to be very close to 2.00. Hence the defect concentration in these ThO_2–UO_2 pellets is very small and consequently the driving force for sintering will be weak, which possibly gives rise to slow sintering. In the ThO_2, ThO_2–2% UO_2 and ThO_2–4% UO_2 pellets, ThO_2 showed larger shrinkage at temperatures higher than 1350 °C, though their O/M ratios were all 2.00. The difference in shrinkage may be associated with very rapid change of oxygen potential near the stoichiometry for uranium bearing pellets.

5.1.2. Air

A density of >92% TD was obtained for ThO_2–UO_2 pellets when sintered in air at 1425 °C for 2 h. Again the effect

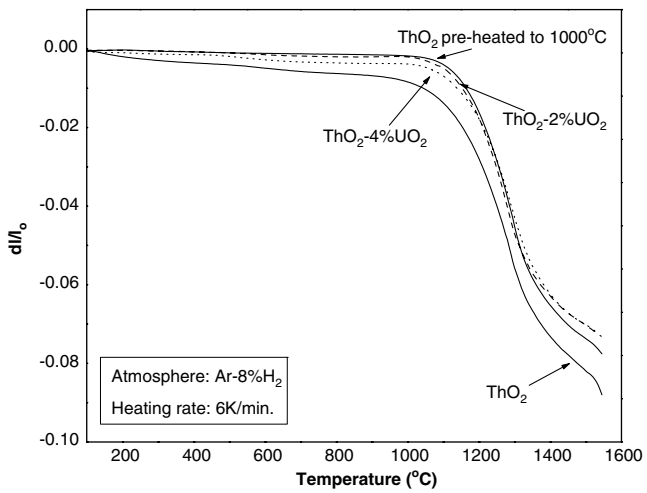

Fig. 9. Shrinkage behaviour on heating in Ar–8% H_2 atmosphere. Curves of ThO_2 (non pre-heated), ThO_2 (pre-heated), ThO_2–2% UO_2 (with pre-heated ThO_2) and ThO_2–4% UO_2 (with pre-heated ThO_2) are shown.

of pre-heating can be clearly noticed from Fig. 10. The ThO_2–2% UO_2 pellet showed only a marginal improvement in shrinkage on comparison with pre-sintered ThO_2 pellet. The shrinkage behaviour of ThO_2–2% UO_2 pellet is almost the same in oxidizing and reducing atmospheres from room temperature to 1350 °C. But above 1350 °C, the ThO_2–2% UO_2 pellet showed larger shrinkage in air than that treated in Ar–8% H_2 atmosphere. From the shrinkage curves of Fig. 6 for ThO_2–4% UO_2 pellet, it is clear that the shrinkage is significantly larger in air than in the reducing atmosphere. The onset temperature of sintering is as low as 800 °C in air. Also, a shrinkage of about 12% is observed in air at the maximum sintering temperature of 1425 °C, while the sintering was only about half of the above value in reducing atmosphere at a higher temperature of 1550 °C. The above behaviour of ThO_2–4% UO_2 pellets in air can be attributed to their higher O/M ratios. The O/M ratios of ThO_2–4% UO_2 pellet were 2.000 and 2.010 in Ar–8% H_2 and in air, respectively (Table 4). Lay and Carter [47] have shown that the self-diffusion coefficient of uranium in UO_{2+x} is proportional to x^2. This is predominantly due to the increased concentration of uranium vacancies in UO_{2+x}. Since the ThO_2–4% UO_2 pellet heated in air has higher O/M ratio than the ThO_2 and ThO_2–2% UO_2 pellets, the larger shrinkage observed for this pellet can be explained by the increased self-diffusion coefficient of uranium.

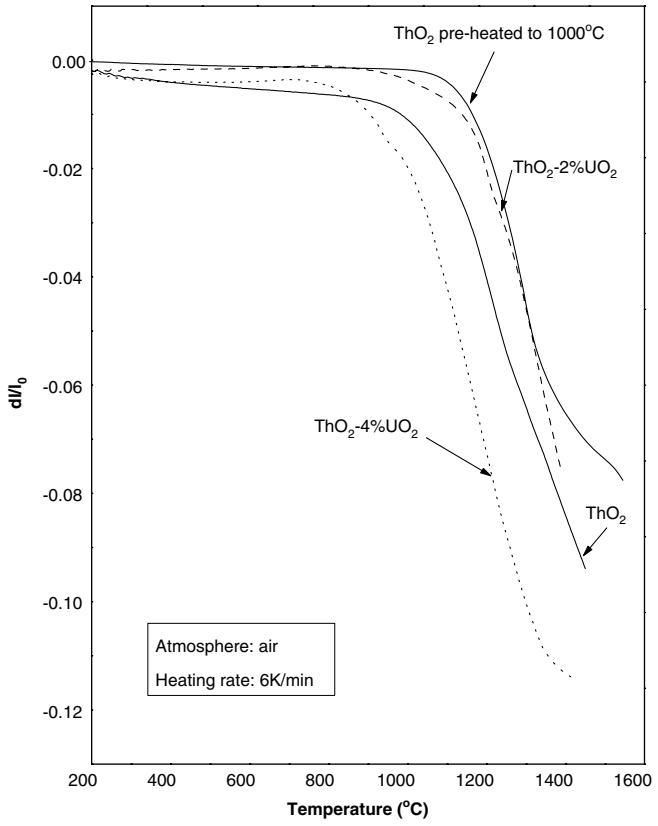

Fig. 10. Shrinkage behaviour on heating in air. Curves of ThO_2 (non pre-heated), ThO_2 (pre-heated), ThO_2–2% UO_2 (with pre-heated ThO_2) and ThO_2–4% UO_2 (with pre-heated ThO_2) are shown.

5.2. Microstructure

The microstructure plays a key role for the fuel behaviour during irradiation, i.e. fission gas release, plasticity, in-pile creep and swelling [48]. The improvement in plasticity and fission gas release can be attained by modifying the microstructures during fabrication [49–51]. The microstructure of ThO_2–2% UO_2 and ThO_2–4% UO_2 pellets obtained in this study was found to be uniform throughout the pellet. In the mixed oxide fuel the presence of fissile rich agglomerates adds complexity to the fuel behaviour. Such agglomerates induce higher local fission rates and consequently higher temperatures, which will lead to cause higher fission gas release and fuel densification in the mixed oxide fuel relative to UO_2 fuel. Hence it is very important to study the distribution of U in the ThO_2 matrix.

The EPMA scanning, which was carried out for ThO_2–4% UO_2 pellet, indicates that the uranium distribution is essentially uniform in the pellet as shown in Fig. 8. But semi-quantitative analysis, which was made by counting the X-rays in a fixed time at six different points from central to peripheral region of the pellet (Table 5) showed that the uranium concentration is higher at the periphery by about 10%, the change being gradual from centre to periphery. The non-homogeneous distribution of uranium in the pellet prepared by impregnation method has been reported by a number of authors [8–11]. This is one of the drawbacks of the impregnation process. A better homogeneity can be attained by using annular pellet. The reason of non-uniform distribution and its effects on the fuel performance can be considered as follows. The impregnation process uses capillary force to draw up the solution into the pores of the host material [8–11]. It may be noted that the maximum concentration of the infiltrate exists at the exterior surface of the substrate. The concentration continuously diminishes from the periphery to the centre of the pellet. Therefore, a continuous concentration gradient of fissile material in the pores of the composite continues to exist after the liquid is removed from the pellet. This concentration gradient continues to exist even after the heat treatment.

The concentration gradient thus obtained during the impregnation process may be beneficial to the nuclear industry by the following reasons [9–11]. The greater concentration of fissile material at the periphery of the pellet will give greater neutron efficiency during operation of a reactor. The neutrons will be able to escape from the pellet more readily as the self-shielding effect is significantly reduced. Also the heat generation will be greater at the

Table 5
Uranium concentrations in the central and peripheral regions of ThO_2–2% UO_2 and ThO_2–4% UO_2 pellets determined by EPMA

Element	ThO_2–2% UO_2 (wt%)	ThO_2–4% UO_2 (wt%)
Centre	2.110	4.010
Periphery	2.390	4.420

pellet periphery and decreases towards the centre of the pellet [29]. For nuclear ceramics having low thermal conductivity values, this phenomenon will be beneficial in the case of an operating incident. The stored thermal energy in the impregnation fuel is significantly lower than that in the conventional fuel where the fissile material is uniformly distributed [9]. This is because the increase in the fuel temperature at the centre of the pellet is significantly depressed in the present fuel.

6. Conclusions

This study has demonstrated that high density ThO_2–2% UO_2 and ThO_2–4% UO_2 pellets can be fabricated by impregnation technique with ThO_2 as the matrix and uranyl nitrate as infiltrant. The densification behaviour of ThO_2, ThO_2–2% UO_2 and ThO_2–4% UO_2 pellets was evaluated using high temperature dilatometry in the atmospheres of Ar–8% H_2 and air. The sintered pellets were characterized by microstructural analysis. The following conclusions were drawn:

(a) The sintering of ThO_2 pellets was retarded by the preheating of green pellets to 1000 °C. At 1400 °C, the shrinkage values were about 7.5% and 6.5% for ThO_2 (non pre-heated) and ThO_2 (pre-heated) pellets, respectively.
(b) The onset temperature of sintering was about 200–250 °C lower for ThO_2–4% UO_2 pellet in oxidizing atmosphere than that in the reducing atmosphere.
(c) The microstructure of ThO_2–2% UO_2 and ThO_2–4% UO_2 pellets showed uniform grain structures.
(d) The EPMA data confirm that uranium concentration was slightly higher at the periphery of the pellet than that at the centre.

References

[1] Hj. Matzke, in: T. Sørensen (Ed.), Non-stoichiometric Oxides, Academic Press, New York, 1981, p. 156.
[2] D.R. Olander, Fundamental Aspects of Nuclear Reactor Fuel Elements, TID-26711-P1, US Department of Energy, 1976, p. 145.
[3] F. Vettraino, G. Magnani, T. La Torretta, E. Marmo, S. Coelli, L. Luzzi, P. Ossi, G. Zappa, J. Nucl. Mater. 274 (1999) 23.
[4] J. Magill, P. Peerani, Hj. Matzke, J. Van Geel, in: IAEA Technical Committee Meeting on Advanced Fuels with Reduced Actinide Generation, 21–23 November, 1995, Vienna.
[5] C. Rubbia, S. Buono, E. Gonzalez, Y. Kadi, J.A. Rubio, European Organization for Nuclear Research, CERN/AT/95-53(ET), 12 December, 1995.
[6] H.A. Feiveson, S.N. Rodionov, Sci. Global Secur. 6 (1997) 265.
[7] Thorium Fuel Cycle – Potentials Benefits and Challenges, IAEA-TECDOC-1450, International Atomic Energy Agency, Vienna, 2005, p. 1.
[8] M.A. Feraday, K.D. Cotnam, F. Preto, Am. Ceram. Soc. Bull. 58 (1979) 21.
[9] R. Lee Harvey, Method of Fabricating Nuclear Fuel, United States Patent No. 4110159, 1978.
[10] Y. Croixmarie, E. Abonneau, A. Fernandez, R.J.M. Konings, F. Desmouliere, L. Donnet, J. Nucl. Mater. 320 (2003) 11.
[11] A. Feraday Melville, Preparation of Mixed Oxide Nuclear Fuel, United States Patent 40201311975, 1975.
[12] M.S. Kazimi, M.J. Driscoll, R.G. Ballinger, K.T. Clarno, K.R. Czerwinski, P. Hejzlar, P.J. LaFond, Y. Long, J.E. Meyer, M.P. Reynard, S.P. Schultz, X. Zhao, Proliferation Resistant, Low Cost, Thoria–Urania Fuel for Light Water Reactors, Annual Report, Nuclear Engineering Department, Massachusetts Institute of Technology, Cambridge, MA, June 1999.
[13] J. Magill, P. Peerani, J. Van Geel, in: Second International ARS Topical Meeting on Advanced Reactor Safety, June 1–4, 1997, Orlando, Florida, 1997.
[14] M.S. Kazimi, E.E. Pilat, M.J. Driscoll, Z. Xu, D. Wang, X. Zhao, in: International Conference on: Back-End of the Fuel Cycle: From Research to Solutions, Global 2001, Paris, France, September 2001.
[15] Philip E. MacDonald, Advanced Proliferation Resistant, Lower Cost Uranium–Thorium Dioxide Fuels for Light Water Reactors, US Department of Energy Nuclear Energy Research Initiative, NERI 99-0153, 1999.
[16] M.S. Kazimi, K. R. Czerwinski, M. J. Driscoll, P. Hejzlar, J.E. Meyer, On the Use of Thorium in Light Water Reactors, MIT-NFC-0016, Nuclear Engineering Department, MIT, April, 1999.
[17] Zhao Xianfeng, M.J. Driscoll, M.S. Kazimi, Trans. Am. Nucl. Soc. 80 (1999) 43.
[18] A. Radkowsky, A. Galperin, Nucl. Technol. 124 (1998).
[19] R.B. Grover, S. Chandra, A Strategy for Growth of Electrical Energy in India, Government of India, Department of Atomic Energy, 2004.
[20] R.K. Sinha, A. Kakodkar, Nucl. Eng. Des. 236 (2006) 683.
[21] R. Chidambharam, Atoms Peace: Int. J. 1 (2006) 137.
[22] D. Haas, J. Somers, A. Renard, A. La Fuente, in: Proceedings Fifth OECD/NEA Information Exchange Meeting on Actinide and Fission Product Partitioning and Transmutation, Mol, Belgium, November, 1998.
[23] A. Fernández, K. Richter, J.C. Closset, S. Fourcaudot, C. Fuchs, J.F. Babelot, R. Voet, J. Somers, in: Proceedings 9th Cimtec-World Forum on New Materials, Symposium VII – Innovative Materials in Advanced Energy Technologies, Part C, 1999, p. 539.
[24] A. Fernández, K. Richter, J. Somers, J. Alloy Comp. 271 (1998) 616.
[25] K. Richter, A. Fernández, J. Somers, J. Nucl. Mater. 249 (1997) 121.
[26] N. Boucharat, A. Fernández, J. Somers, R.J.M. Konings, D. Haas, in: Proceedings of the 6th IMF Workshop, Strassbourg, June, 2000.
[27] A. Fernandez, K. Richter, J. Somers, Preparation of spinel ($MgAl_2O_4$) spheres by a hybrid sol–gel technique, in: 9th Cimtec-World Ceramics Congress, Advanced in Science and Technology, vol. 15, Ceramics: Getting into the 2000's. Part C, 1999.
[28] K. Richter, A. Fernandez, J. Somers, J. Nucl. Mater. 249 (1997) 121.
[29] A. Fernandez, D. Haas, R.J.M. Konings, J. Somers, J. Am. Ceram. Soc. 85 (2002) 694.
[30] U. Basak, S. Mishra, M.R. Nair, R. Ramachandran, S. Majumdar, H.S. Kamath, in: Proceedings of Characterization and Quality Control of Nuclear Fuels, CQCNF-2002, Hyderabad, p. 196.
[31] Hj. Matzke, J. Chem. Soc. Faraday Trans. 86 (1990) 1243.
[32] F. Thummler, W. Thomma, Metall. Rev. 115 (1967) 69.
[33] R.L. Coble, J.E. Burke, in: J.E. Burke (Ed.), Progress in Ceramic Science, vol. 3, Pergamon, Oxford, 1963, p. 197.
[34] M. Mayo, Int. Mater. Rev. 41 (3) (1996) 85.
[35] H. Palmour, D.R. Johnson, in: G.C. Kuczynski, N.A. Hooton, C.F. Gibbs (Eds.), Sintering and related Phenomena, Gordon and Breach, New York, 1967, p. 779.
[36] D.L. Johnson, T.M. Clarke, Acta Met. 12 (1964) 1173.
[37] R.L. Coble, J. Am. Ceram. Soc. 41 (1958) 55.
[38] D.L. Johnson, I.B. Cutler, J. Am. Ceram. Soc. 46 (1963) 541.
[39] W.D. Kingery, M. Berg, J. Appl. Phys. 26 (1955) 1205.
[40] L. Berrin, D.L. Johnson, in: G.C. Kuczynski, N.A. Hooton, C.F. Gibbs (Eds.), Sintering and Related Phenomena, Gordon and Breach, New York, 1967, p. 369.
[41] D.L. Johnson, J. Appl. Phys. 40 (1969) 192.

[42] M.H. RandThorium: Physico-chemical Properties of its Compounds and Alloys, Atomic Energy Review, IAEA, Vienna, 1975, p. 7, Special issue no. 5.
[43] J.R. Mathews, J. Chem. Soc. Faraday Trans. 83 (2) (1987) 1273.
[44] R.W. Cahn, P. Haasen, E.J. Krammer, B.R.T. FrostMaterials Science and Technology, A Comprehensive Review, vol. 10A, VCH Publishers, New York, 1994, p. 114.
[45] C.R.A. Catlow, J. Chem. Soc. Faraday Trans. 83 (1987) 1065.
[46] C.R.A. Catlow, A.B. LidiardProceedings of Symposium on Thermodynamics of Reactor Materials, vol. II, IAEA, Vienna, 1974, p. 27.
[47] K.W. Lay, R.E. Carter, J. Nucl. Mater. 30 (1969) 74.
[48] K.C. Radford, J.M. Pope, J. Nucl. Mater. 116 (1983) 305.
[49] K. Maeda, K. Katsuyama, T. Asaga, J. Nucl. Mater. 346 (2005) 244.
[50] U.M. El-Saied, D.R. Olander, J. Nucl. Mater. 207 (1993) 313.
[51] J.A. Turnbull, C.A. Friskney, J. Nucl. Mater. 71 (1978) 238.